



REGULAR ARTICLE

# FeSTAR2 interacted by FeSTAR1 alters its subcellular location and regulates Al tolerance in buckwheat

Jia Meng Xu · Zhan Qi Wang · Jian Feng Jin ·

Wei Wei Chen · Wei Fan · Shao Jian Zheng ·

Jian Li Yang

Received: 2 September 2018 / Accepted: 10 January 2019

© Springer Nature Switzerland AG 2019

## Abstract

**Aims** Buckwheat (*Fagopyrum esculentum*) exhibits high Al tolerance, but only a few genes have been functionally characterized. We previously characterized a half-type ABC transporter, *Fagopyrum esculentum* sensitive to Al rhizotoxicity1 (FeSTAR1), in buckwheat

---

Responsible Editor: Juan Barcelo.

**Electronic supplementary material** The online version of this article (<https://doi.org/10.1007/s11104-019-03943-z>) contains supplementary material, which is available to authorized users.

J. M. Xu · J. F. Jin · S. J. Zheng · J. L. Yang (✉)  
State Key Laboratory of Plant Physiology and Biochemistry,  
College of Life Sciences, Zhejiang University, Hangzhou 310058,  
China  
e-mail: yangjianli@zju.edu.cn

Z. Q. Wang  
Key Laboratory of Vector Biology and Pathogen Control of  
Zhejiang Province, College of Life Sciences, Huzhou University,  
Huzhou 313000, China

W. W. Chen  
Research Centre for Plant RNA Signaling, Institute of Life  
Sciences, College of Life and Environmental Sciences, Hangzhou  
Normal University, Hangzhou 310036, China

W. Fan  
State Key Laboratory of Conservation and Utilization of  
Bio-resources in Yunnan, The Key Laboratory of Medicinal Plant  
Biology of Yunnan Province, National & Local Joint Engineering  
Research Center on Germplasm Innovation & Utilization of  
Chinese Medicinal Materials in Southwest China, Yunnan  
Agricultural University, Kunming 650201, China

Al tolerance. This study aims to investigate whether and how another half-type ABC transporter (FeSTAR2) plays role in Al tolerance in buckwheat.

**Methods** The expression of *FeSTAR2* and complementation test in *Arabidopsis als3* mutant was examined. The interaction between FeSTAR1 and FeSTAR2 and subcellular location were analyzed by bimolecular fluorescence complementation (BiFC) and yeast two-hybrid (Y2H) assays.

**Results** Al rapidly and specifically induced *FeSTAR2* expression. Having transmembrane domains, FeSTAR2 localizes to membrane. BiFC and Y2H assays showed that FeSTAR2 could interact with FeSTAR1 which contains only nucleotide binding domain. Intriguingly, interaction between FeSTAR1 and FeSTAR2 altered their locations. Both heterologous expression of *FeSTAR2* in *als3* and exogenous UDP-glucose rescued its Al hypersensitivity of *als3* mutant, suggesting that involvement of FeSTAR2 in Al tolerance requires UDP-glucose. Furthermore, Al-induced inhibition of xyloglucan endotransglucosylase (XET) activity in both *atstar1* and *als3* mutants could be restored by UDP-glucose.

**Conclusion** Our results indicate that FeSTAR2 interacts with FeSTAR1 to form an ABC transporter to regulate Al tolerance by vesicular transport of UDP-glucose which affects hemicellulose metabolism by regulating XET activity.

**Keywords** Aluminum toxicity · Cell wall · Protein interaction · UDP-glucose · Xyloglucan

## Introduction

Buckwheat (*Fagopyrum esculentum* Moench) is highly tolerant to Al stress which is one of the major factors limiting plant productivity on acid soils (Kochian et al. 2004; Ma et al. 1997). During the last two decades, considerable progresses have been made toward unraveling the physiological mechanisms of Al tolerance in buckwheat. Upon Al exposure, root tip of buckwheat could secrete oxalate and citrate rapidly to chelate rhizospheric Al (Klug and Horst 2010; Zheng et al. 1998, 2005; Lei et al. 2017b). A portion of rhizospheric ionic Al can be taken up actively by root tip of buckwheat to further reduce apoplastic Al concentrations (Ma and Hiradate 2000). Once entered into cytoplasm, Al is compartmentalized into vacuoles and chelated with oxalate at a 1:3 Al-oxalate ratio (Ma et al. 1998). As an Al-accumulating plant species, buckwheat is able to transport Al from the roots to the shoots in the form of Al-citrate complex (Ma and Hiradate 2000). After reaching leaves, Al can be compartmentalized into leaf vacuoles and complexed by oxalate and citrate (Shen et al. 2002, 2004).

Recent progress in genome sequence greatly facilitates the cloning and characterization of genes involved in buckwheat Al tolerance (Yokosho et al. 2014; Zhu et al. 2015; Chen et al. 2017; Xu et al. 2017). For example, an ATP-binding cassette (ABC) transporter-like gene *FeALS3* (*Fagopyrum esculentum ALUSMINUM SENSITIVE 3*), which is also known as *FeSTAR2* (*Fagopyrum esculentum Sensitive to Aluminum Rhizotoxicity2*; Zhu et al. 2015; Xu et al. 2017; Che et al. 2018), has been reported to be involved in Al resistance (Reyna-Llorens et al. 2015), but its biological functions has to be investigated. *ALS3* in *Arabidopsis* was for the first time reported to be involved in Al tolerance possibly functioning to redistribute accumulated Al away from sensitive tissues (Larsen et al. 2005). Later, rice *OsSTAR2* displaying sequence similarity with *Arabidopsis ALS3* was characterized being implicated in Al tolerance by forming a complex protein with *OsSTAR1* (Huang et al. 2009). *FeIREG1* (*Fagopyrum esculentum IRON REGULATED 1*) is a tonoplast-localized transporter involved in vacuolar sequestration of Al into root cells (Yokosho et al. 2016). However, *FeIREG1* is only expressed in roots but not in leaves. Recently, Lei et al. (2017a) identified two half-size ABC transporter genes, *FeALS1.1* (*Fagopyrum esculentum ALUSMINUM SENSITIVE 1.1*) and *FeALS1.2*, encoding tonoplast-localized transporters for

Al sequestration. Both *FeALS1.1* and *FeALS1.2* are homologous to rice *OsALS1* (Huang et al. 2012). Subsequently, two *MATE* (*Fagopyrum esculentum Multi-drug and Toxic Compound Extrusion*) genes were further identified by Lei et al. (2017b). Members from *MATE* gene family have been demonstrated to be responsible for Al-induced citrate secretion in a number of plant species (Furukawa et al. 2007; Magalhaes et al. 2007; Yang et al. 2011a; Liu et al. 2018). Lei et al. (2017b) reported that *FeMATE1* is responsible for Al-induced citrate secretion from roots, while *FeMATE2* is probably related to transport citrate into golgi system for the internal detoxification of Al. More recently, *FeSTAR1* was functionally characterized with respect to Al tolerance in buckwheat (Che et al. 2018; Xu et al. 2018). *FeSTAR1* has a similar function as *AtSTAR1* because introduction of *FeSTAR1* into *atstar1* mutant rescued its sensitivity to Al (Huang et al. 2010; Xu et al. 2018). However, *FeSTAR1* was found to be localized at cytoplasm and nucleus, and contains only nucleotide binding domain (Xu et al. 2018). It seems that *FeSTAR1* alone is insufficient to modify cell wall properties under Al stress.

In rice, the complex protein of *OsSTAR1* and *OsSTAR2* is localized to vesicles and is able to transport UDP-glucose to the apoplast presumably for modifying the Al-sensitive part of cell walls (Huang et al. 2009). However, Dong et al. (2017) reported that the complex protein of *Arabidopsis AtSTAR1* and *ALS3* is mainly localized to tonoplast. Although the complex protein of *AtSTAR1* and *ALS3* mediates anion efflux, it is not able to transport UDP-glucose (Dong et al. 2017). The latest report indicated that *FeSTAR1* could interact with *FeSTAR2* when introduced both proteins in onion epidermal cells (Che et al. 2018). Furthermore, the localization of *FeSTAR1* was changed to the membrane from its original cytoplasmic location (Che et al. 2018). It is therefore very likely that *FeSTAR1* works with *FeSTAR2* to modify cell walls in response to Al stress. However, how *FeSTAR2* is involved in Al tolerance remains unclear.

On the basis of comparative transcriptomic analysis of the root apex and the leaves of buckwheat in response to Al, we identified five transporter genes, *FeMATE1*, *FeALS1*, *FeSTAR1*, *FeSTAR2*, and a divalent ion transporter gene being up-regulated by Al in both roots and leaves (Chen et al. 2017; Xu et al. 2017). In the present study, we investigated the expression pattern, subcellular localization, and function of *FeSTAR2*. We also examined the interaction between *STAR1* and *STAR2* proteins from different plant species. Our results showed

that FeSTAR2 seems to be localized to vesicles. However, its subcellular location was altered by forming a complex protein with FeSTAR1. FeSTAR2 could complement the Al-sensitive phenotype of *als3* mutant when exposed to Al stress. We further demonstrated that UDP-glucose is involved in STAR2-mediated Al resistance by regulating the XET activity.

## Materials and methods

### Plant materials and treatments

The buckwheat (*Fagopyrum esculentum* Moench. cv. Jiangxi) seeds were germinated at 26 °C in the dark after sterilization with 5% (v/v) NaClO for 10 min and soak in water overnight. The germinated seeds were cultured in 0.5 mM CaCl<sub>2</sub> solution (pH 4.5) for subsequent Al stress treatments. For dose-response experiment, 3-day-old seedlings were subjected to 0.5 mM CaCl<sub>2</sub> solution (pH 4.5) containing 0, 10, 20, 40, or 60 μM AlCl<sub>3</sub> for 24 h. For time-course experiment, 3-day-old seedlings were exposed to 0.5 mM CaCl<sub>2</sub> solution with 20 μM AlCl<sub>3</sub> for 0, 3, 6, 12, or 24 h. For specificity analysis, 3-day-old seedlings were exposed to 0.5 mM CaCl<sub>2</sub> solution containing 20 μM AlCl<sub>3</sub>, 1 μM CuCl<sub>2</sub>, 20 μM CdCl<sub>2</sub> or 20 μM LaCl<sub>3</sub> for 24 h. All the above experiments were carried out in an environmentally controlled growth room with a 14 h/26 °C day (light intensity of 300 μmol photons m<sup>-2</sup> s<sup>-1</sup>) and a 10 h/22 °C night regime.

The Arabidopsis mutant *als3* (SALK\_004094) was kindly provided by Dr. Dong Liu (Tsing Hua University, China). The genetic background of Arabidopsis materials used in our study was Col-0 ecotype. For root growth analysis, the seeds were germinated and grown on 1/2 MS medium (Pi concentration reduced to 100 μM, pH 4.5, solid with 0.8% agar) containing 0 or 300 μM Al for a week. Then the primary root length was measured with a ruler after treatment. For investigate the effects of exogenous UDP-glucose on Al-induced root growth inhibition in both wild type and the mutants *atstar1* and *als3*, 500 μM sterilized UDP-glucose (sigma) were added or not added to the 1/2 MS medium containing 0 or 300 μM Al and then the seeds were germinated and grown on the plates for a week. The Arabidopsis were cultured in a plant incubator with a daytime 16 h/24 °C (light intensity of 300 mmol photons m<sup>-2</sup> s<sup>-1</sup>) and 8 h/22 °C night regime.

### RNA extraction and RT-PCR analysis

RNA isolation from buckwheat and Arabidopsis were carried out by respectively using RNeasy Mini Kit (Qiagen) and MiniBEST Universal RNA Extraction Kit (TAKARA). Both real-time quantitative RT-PCR analysis of *FeSTAR2* expression in buckwheat under Al stress and semi-quantitative RT-PCR assay of determining *FeSTAR2* expression level in transgenic Arabidopsis lines were performed as described by Xu et al. (2018). Primers used for RT-PCR were listed in supplemental Table S1.

### Transgenic Arabidopsis lines construction

The amplified *FeSTAR2* coding sequence with or without the stop codon was cloned in-frame in front of the GFP coding region in the modified pCAMBIA1300 vector, thus obtaining 35S::*FeSTAR2*, 35S::*FeSTAR2-GFP*. The vectors were respectively introduced into Arabidopsis wild-type (Col-0) and *als3* mutant by agrobacterium-mediated transformation to generate *FeSTAR2OE* (for gene function characterization), 35S::*FeSTAR2-GFP* (for subcellular localization) and 35S::*FeSTAR2/als3* transgenic lines (Comp#1 and Comp#2).

A 1968 bp promoter sequence of *FeSTAR2* was obtained by genome walking using the Genome Walker Universal Kit (Clontech Laboratories) with primers listed in supplemental Table S1 according to Xu et al. (2018). The 1968 bp 5'-upstream regions of *FeSTAR2* was amplified from genome of buckwheat, then cloned to pCAMBIA1301 vector and introduced into Arabidopsis wild-type (Col-0) plants by agrobacterium-mediated transformation to result in *FeSTAR2p::GUS* transgenic lines.

### β-Glucuronidase analysis

Seedlings of transgenic GUS reporter lines treated with or without 7 μM Al according to Xu et al. (2018). GUS staining was performed according to previous report (Jefferson et al. 1987).

### Subcellular localization

*FeSTAR2-GFP* fusion over-expressed transiently in tobacco (*N. benthamiana*) leaves or stably in Arabidopsis for FeSTAR2 subcellular localization analysis. *FeSTAR1-GFP* fusion and *FeSTAR2-mCherry* fusion (cloned into the modified pCAMBIA 1300 vector with

a mCherry tag) together over-expressed transiently in *N. benthamiana* leaves for interaction analysis. GFP or mCherry fluorescence signals were observed using confocal laser scanning microscopy (LSM710; Carl Zeiss, Jena, Germany).

#### Bimolecular fluorescence complementation (BiFC) assay

The full-length coding sequences of *FeSTAR1* and *FeSTAR2* were amplified, and cloned into p2YN or p2YC as a fusion with the N-terminal or C-terminal fragment of YFP (Zhong et al. 2017), resulting in FeSTAR1-YFP<sup>N</sup>, and FeSTAR2-YFP<sup>C</sup>. The resulting constructs were transiently transformed into *N. benthamiana* leaves by *Agrobacterium tumefaciens* GV3101 infiltration. For co-localization analysis, endoplasmic reticulum (ER) marker, ER-rk CD3–960 and tonoplast marker, vac-rk CD3–975 were included for co-transformation (Nelson et al. 2007). YFP fluorescence was observed and photographed by confocal microscopy (LSM710; Carl Zeiss, Jena, Germany) at 48–72 h after infiltration. Primers used for construction of BiFC vectors were listed in supplemental Table S1.

#### Split-ubiquitin yeast two-hybrid (Y2H) analysis

The Y2H assay was carried out using the DUAL membrane System (Biotech Dualsystems). The full-length coding sequence of *FeSTAR2*, *OsSTAR2* and *ALS3* were amplified and then fused with the C-terminal half of ubiquitin (Cub) to generate the constructs FeSTAR2-Cub, OsSTAR2-Cub and ALS3-Cub as the preys. The coding regions of *FeSTAR1*, *OsSTAR1* and *AtSTAR1* were amplified and fused with the mutated N-terminal half of ubiquitin (NubG), resulting in the constructs FeSTAR1-NubG, OsSTAR1-NubG and AtSTAR1-NubG as the baits. Different combinations of preys and baits were co-transformed into NMY51 yeast cells. The transformants were selected on dropout medium without Leu and Trp. Then the protein-protein interactions were assessed by the growth of yeast colonies on synthetic medium lacking Leu, Trp, His, and Ade at 30 °C for 3 days.

#### XET activity assay

The XET action of xyloglucan endotransglucosylase/hydrolases (XTH) was determined according to Vissenberg et al. (2000). Seven-day-old seedling roots

were incubated in a 6.5 μm XGO-SR mixture (XLLG-SR > XXLG-SR > XXXG-SR; for nomenclature, see Fry et al. 1993; for the synthesis, see Fry 1997) dissolved in 25 mM MES buffer at pH 5.5 for 1 h. The assay was followed by a 10-min wash in ethanol:formic acid:water (15:1:4, v/v/v) to remove any remaining unreacted XGO-SRs; a further incubation overnight in 5% formic acid was performed to remove apoplastic, non-wall-bound XGO-SRs. Samples were mounted on glass slides and examined with a laser-scanning confocal microscope (LSM 510; Zeiss) using excitation light of 540 nm.

#### Phylogenetic analysis

We constructed neighbor-joining (NJ) trees using the MEGA software (version 7.0) (<http://www.megasoftware.net>) (Kumar et al. 2016) with the following parameters: Poisson correction, pairwise deletion, and bootstrap (1000 replicates; random seed). This was performed as previously described by Wang et al. (2015).

#### Statistical analysis

Statistical analyses were conducted by Tukey's test among treatments or one-way ANOVA test between genotypes ( $P < 0.05$ ) with DPS 11.0 edition for windows (Tang and Zhang 2012).

## Results

#### Isolation and sequence analysis of *FeSTAR2* in buckwheat

Based on the sequence information from previous transcriptomic analysis of buckwheat (Xu et al. 2017), we designed gene-specific primers to check the accuracy of *FeSTAR2* cDNA by sequencing the PCR product. The *FeSTAR2* coding region is 795 bp in length, and encodes a protein of 264 amino acids (GenBank accession no. MH827970; Fig. 1a). To examine the evolutionary relationship among STAR2 proteins from various plant species, we performed a sequence alignment. The result showed that *FeSTAR2*, *ALS3* and *OsSTAR2* display a high sequence similarity (Fig. 1a). Topological surveys based on the HMMTOP program (<http://www.enzim.hu/hmmtop>) indicated that STAR2 proteins have

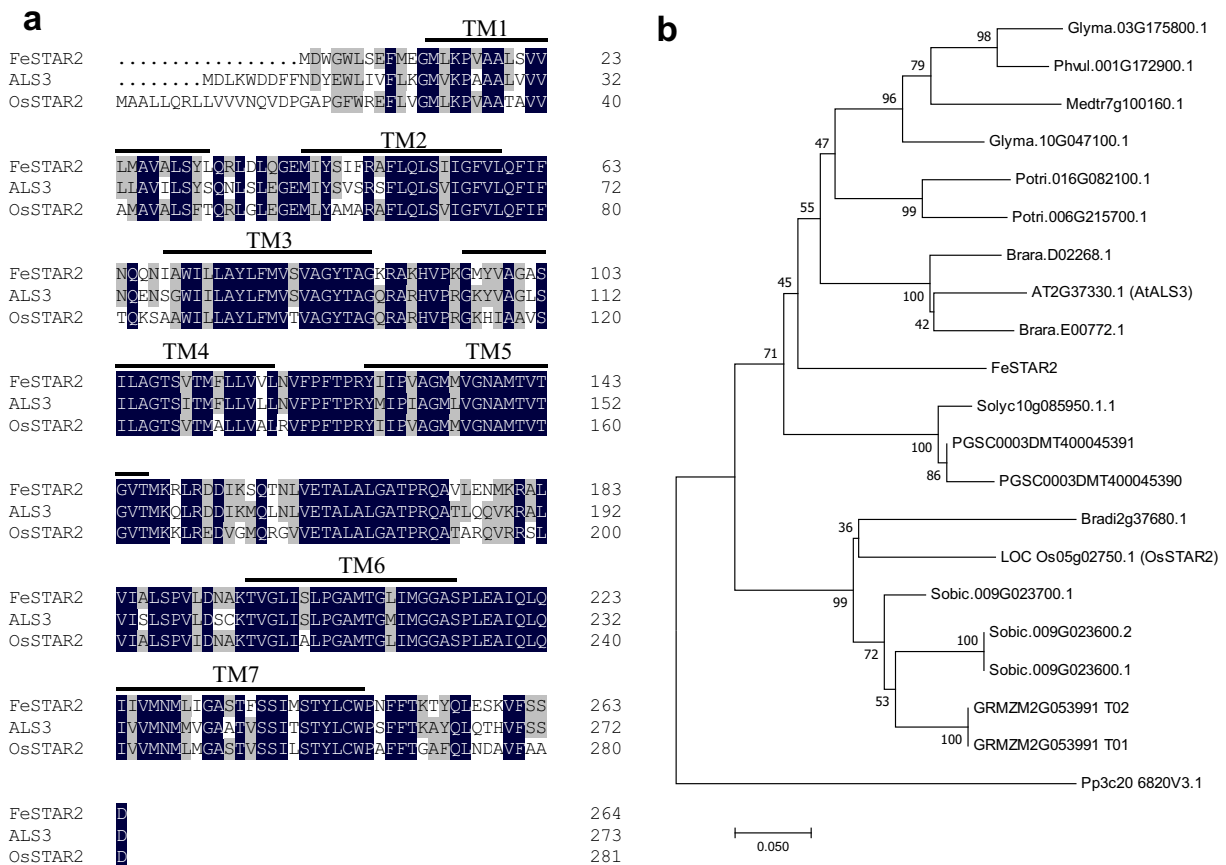


**Fig. 1 Sequence analysis of *FeSTAR2*. a** Amino acid sequence alignment of STAR2 proteins from buckwheat (FeSTAR2), rice (OsSTAR2; LOC\_Os05g02754), and Arabidopsis (ALS3; At2g37330). **b** Phylogenetic analysis of FeSTAR2 and its 20 close

homologs. The numbers under the branches refer to the bootstrap value of the neighbor-joining phylogenetic tree. The length of the branches is proportional to the amino acid variation rates. The scale bar indicates the number of amino acid substitutions per site

7 transmembrane domains, suggesting that they are membrane-localized proteins (Fig. 1a). Phylogenetic relationship analysis indicated that FeSTAR2 was more closely related to Arabidopsis ALS3 than rice OsSTAR2 (Fig. 1b).

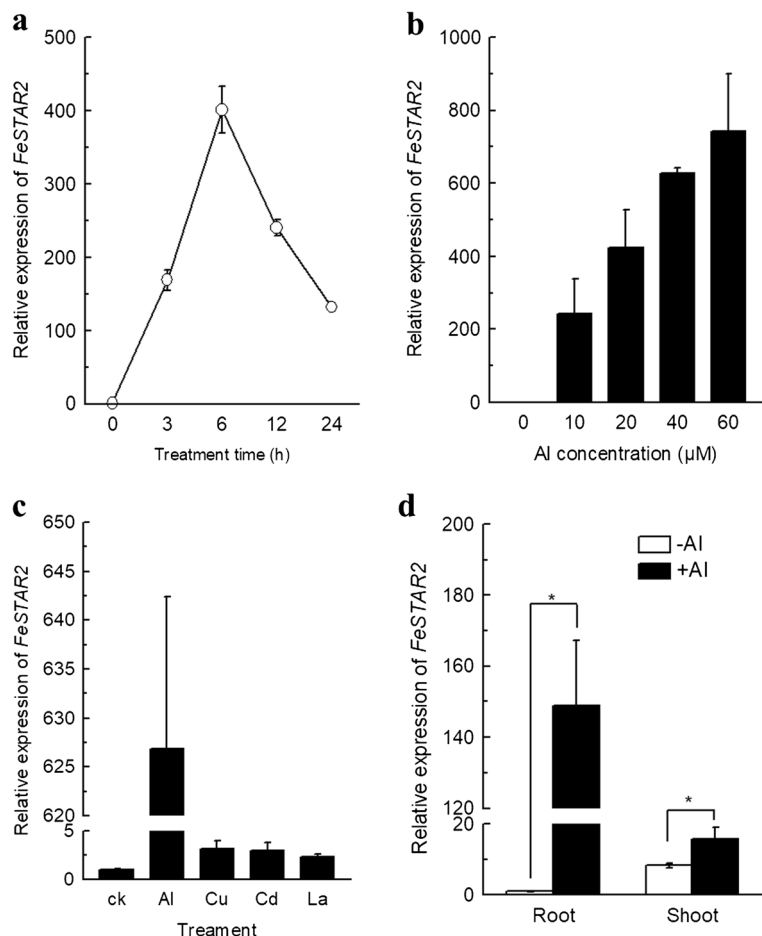
#### Expression pattern of *FeSTAR2*

Time-course experiment showed that the expression of *FeSTAR2* was dramatically induced by Al stress after 3 h of exposure and maximized at 6 h. Thereafter, the expression of *FeSTAR2* dropped down, but there remained more than 100-fold increase after 24 h of exposure (Fig. 2a). In a dose-response experiment, the expression of *FeSTAR2* increased with increasing Al concentrations after 6 h of exposure (Fig. 2b). Other metals could induce *FeSTAR2* expression slightly, but the induction was significantly lower than that induced by Al stress

(Fig. 2c). We next examined spatial expression of *FeSTAR2* with or without Al stress. Consistent with our previous RNA-seq analysis, the expression of *FeSTAR2* was responsive to Al not only in roots but also in leaves (Fig. 2d).

To further investigate the tissue-specific localization of *FeSTAR2* expression, a 1968-bp DNA sequence upstream of the translation start codon (ATG) was isolated from buckwheat (Fig. S1). This promoter fragment was fused to a GUS reporter gene and transformed into Arabidopsis wild-type (WT) plants. As shown in Fig. S2, GUS activity was observed in the whole plants in the absence of Al stress. In root tip, GUS activity was predominately observed in root cap and elongation region but not in meristem and transition zone between meristem and elongation zone. However, Al stress induced GUS activity strongly at both meristem and transition zone (Fig. S2).

**Fig. 2 Expression pattern of *FeSTAR2*.** **a** time-course analysis of *FeSTAR2* expression in the root tip (0–1 cm) of buckwheat in response to 0.5 mM CaCl<sub>2</sub> solution (pH 4.5) containing 20 μM Al treatment. **b** dose-response of *FeSTAR2* expression to 0.5 mM CaCl<sub>2</sub> solution (pH 4.5) containing different concentrations of AlCl<sub>3</sub> for 6 h in the root tip (0–1 cm) of buckwheat. **c** specificity of *FeSTAR2* expression to Al in the root tip (0–1 cm) of buckwheat. Concentrations of Al (20 μM), Cu (1 μM), Cd (20 μM) or La (20 μM) in 0.5 mM CaCl<sub>2</sub> solution (pH 4.5) were used. Treatment was conducted for 6 h. **d** the expression level of *FeSTAR2* in the root and leaf of buckwheat under 0.5 mM CaCl<sub>2</sub> solution (pH 4.5) containing 20 μM Al treated for 6 h. Data in (a) to (d) represent the mean ± SD of three biological replicates each with three technical replicates



### Subcellular location of FeSTAR2

To examine the subcellular location of FeSTAR2, we first transiently expressed FeSTAR2-GFP fusion protein in *N. benthamiana* leaves. The GFP fluorescence appears punctiform, ellipse, and columnar in epidermal cells of *N. benthamiana* (Fig. 3a). We next stably expressed FeSTAR2-GFP fusion protein in Arabidopsis. Similar pattern of GFP signals was observed in transgenic Arabidopsis roots (Fig. 3b). Although it is hard to precisely locate FeSTAR2, it can be deduced that FeSTAR2 is located at biomembranes because it contains 7 transmembrane domains (Fig. 1a).

### Interaction between FeSTAR1 and FeSTAR2

OsSTAR1 and OsSTAR2 proteins in rice and AtSTAR1 and ALS3 proteins in Arabidopsis could interact with each other (Huang et al. 2009; Dong et al. 2017). We

therefore wonder whether FeSTAR1 and FeSTAR2 could form a complex protein. To test this possibility, we carried out a split-ubiquitin Y2H analysis. STAR1 protein could interact with its respective STAR2 protein from each plant species (Fig. 4). Interestingly, STAR1 and STAR2 proteins could interact with each other in spite of their origins (Fig. 4). The present result suggests that STAR1 and STAR2 proteins are structurally and functionally highly conserved among different plant species.

Interaction of STAR1 and STAR2 changed their subcellular locations

FeSTAR1 is a soluble protein and localized to cytoplasm and nucleus (Che et al. 2018; Xu et al. 2018), whereas FeSTAR2 has transmembrane domains (Fig. 3). The different locations led us to wonder whether interaction between STAR1 and STAR2 will result in

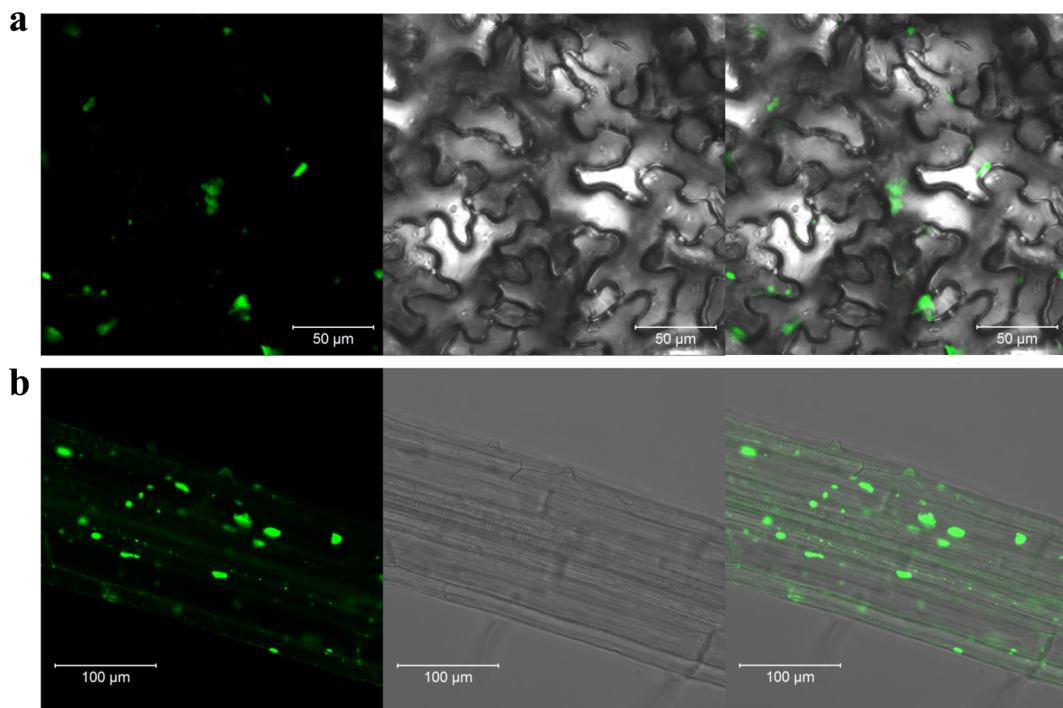
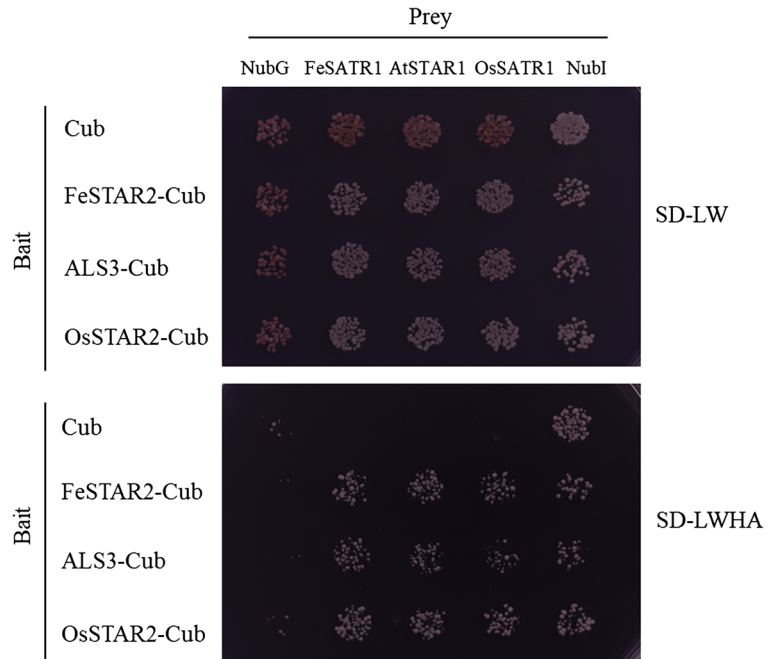


**Fig. 3** Subcellular location of FeSTAR2 protein. **a** *35S::FeSTAR2-GFP* was transiently expressed in *N. benthamiana* leaves. **b** *35S::FeSTAR2-GFP* was stably expressed in *Arabidopsis* root. Bar = 50  $\mu$ m in (a) and 100  $\mu$ m in (b)

**Fig. 4** Split-ubiquitin yeast two-hybrid (Y2H) analysis of interaction between STAR1 and STAR2 proteins. Cub is the C-terminal ubiquitin, the protein of interest fused with Cub as bait; NubI and NubG are, respectively, the wild type and mutated N-terminal fragment of ubiquitin, the other objective protein fused to NubI as prey. Different combinations of prey and bait vectors are transformed to NMY51 yeast cells and then the yeast grown on SD-Leu-Trp (SD-LW)/SD-Leu-Trp-His-Ade (SD-LWHA) media at 30 °C for 3 days



changes in their locations. To this end, we performed a BiFC assay as described previously (Zhong et al. 2017). We found that FeSTAR1 and FeSTAR2 could interact with each other in our BiFC system. Interestingly, the complex protein of FeSTAR1 and FeSTAR2 seems to be localized at both plasma membrane and vesicles, because the signal was not merged with both ER marker and tonoplast marker (Fig. 5).

To further confirm that interaction of FeSTAR1 and FeSTAR2 could alter their location, we transiently co-expressed both FeSTAR1-GFP and FeSTAR2-mCherry fusion proteins into *N. benthamiana* leaves (Fig. 6). Our previous study showed that FeSTAR1 localizes to cytoplasm and nucleus (Xu et al. 2018) and FeSTAR2 localizes to vesicles (Fig. 3). However, their subcellular locations changed to membrane when both fusion proteins were co-expressed in *N. benthamiana* leaves (Fig. 6). These results indicate that interaction between STAR1 and STAR2 proteins result in changes in their subcellular localization.

#### Complementation of *als3* mutants with FeSTAR2

To further examine the role of FeSTAR2 with respect to Al tolerance, Arabidopsis *als3* mutant was used to perform complementation test. We transformed FeSTAR2 into *als3* mutant under the control of 35S CaMV promoter. RT-PCR analysis showed that *FeSTAR2* was

transcriptionally expressed in two independent transgenic lines (Comp.#1 and Comp.#2), whereas it was absent in both WT and *als3* mutant plants (Fig. 7a). In the absence of Al, the root growth was similar among different genotypes (Fig. 7b). While the roots of *als3* were more severely inhibited than that of WT, those of the two complemented lines were similar with WT (Fig. 7b). The relative root elongation was inhibited by about 70% in *als3*, but that of WT as well as two complemented lines was only inhibited by around 40% (Fig. 7c). These results suggest that buckwheat FeSTAR2 is a functional homolog of Arabidopsis ALS3 in terms of Al tolerance.

#### Exogenous UDP-glucose recovers *als3* Al sensitivity

Exogenous applied UDP-glucose could alleviate significantly the Al-induced root growth inhibition of rice *osstar1* and *osstar2* mutants (Huang et al. 2009). Recently, we also demonstrated that buckwheat FeSTAR1-mediated Al tolerance is associated with UDP-glucose metabolism (Xu et al. 2018). We therefore wanted to know whether FeSTAR2-mediated Al tolerance is related to UDP-glucose too. In the absence of Al, UDP-glucose did not affect root growth of WT or mutants (Fig. 8a). However, in the presence of Al, exogenous UDP-glucose significantly alleviated the Al-induced

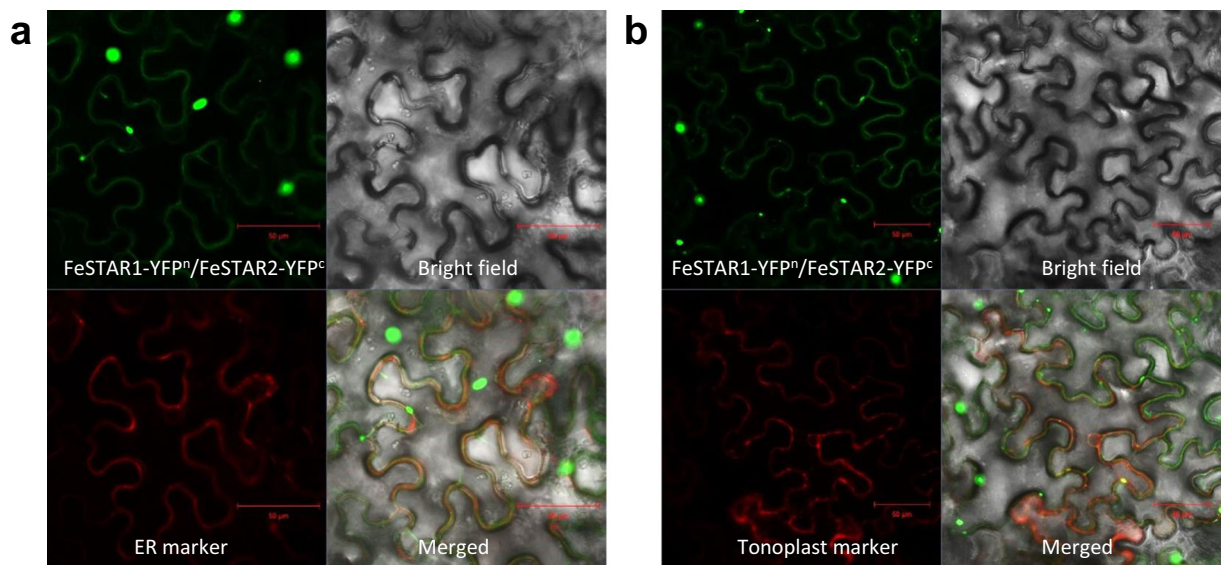
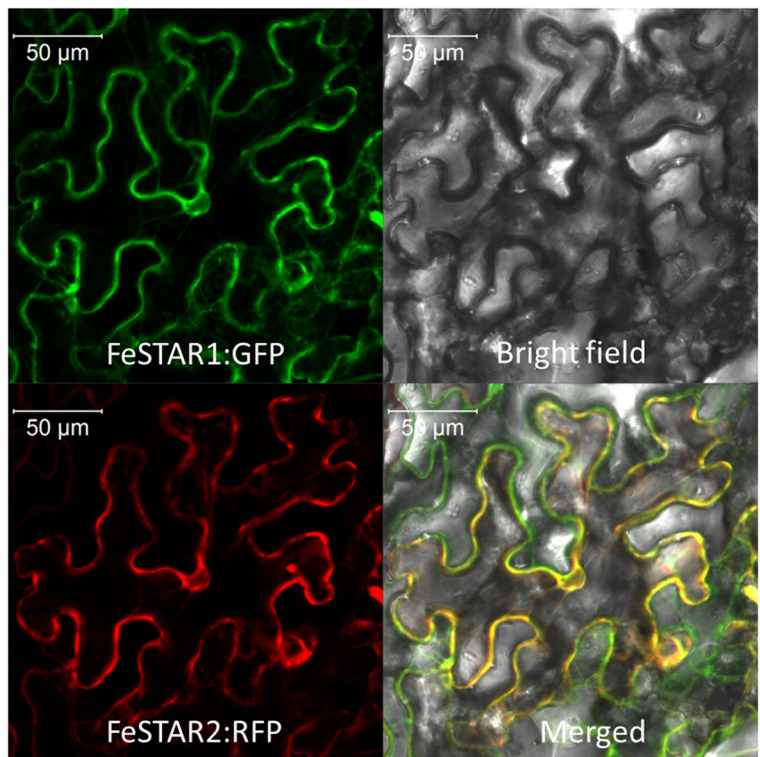


**Fig. 5** Bimolecular fluorescence complementation (BiFC) analysis of interaction between STAR1 and STAR2 proteins. FeSTAR1-YFP<sup>N</sup>, and FeSTAR2-YFP<sup>C</sup> fusion proteins were co-

expressed in the leaves of *N. benthamiana*. ER marker (ER-rk CD3–960) and tonoplast marker (vac-rk CD3–975) were used for co-localization analysis

**Fig. 6 Localization of FeSTAR2 changed by interacting with FeSTAR1.** Both 3SS::FeSTAR1-GFP and 3SS::FeSTAR2-mCherry were transiently co-expressed in *N. benthamiana* leaves



inhibition of root growth in the mutant plants (Fig. 8b). These results suggest that UDP-glucose is involved in STAR2-mediated Al resistance.

#### Exogenous UDP-glucose restores XET activity of *atstar1* and *als3* mutants under Al stress

We have previously demonstrated that STAR1-mediated Al tolerance is associated with hemicellulose (HC) metabolism (Xu et al. 2018). The similar effect of UDP-glucose on Al tolerance in both *atstar1* and *als3* mutants suggest that the same mechanism might be shared by both STAR1 and STAR2 proteins. In dicotyledonous plant species, xyloglucan is the most abundant HC and XTHs are critical for xyloglucan metabolism by catalyzing molecular grafting and/or hydrolysis of xyloglucan (Rose et al. 2002). Here, we used the fluorescently labeled xyloglucan oligosaccharides (XGO-SRs) to visualize the activity of XET (Vissenberg et al. 2000, 2003). In the absence of Al, there was no significant difference in XET activity between WT and *atstar1* or *als3* mutants irrespective of being treated with or without UDP-glucose. Al stress dramatically inhibited XET activity in WT plants and the inhibition was more evident in both mutants. Interestingly, exogenous UDP-glucose could

restore XET activity of both mutants to the level of WT plants, whereas it could not further improve XET activity in WT plants in the absence of Al (Fig. 9). These results suggest that STAR1/2-mediated Al tolerance is associated HC metabolism which is regulated by UDP-glucose-mediated XET activity.

#### Discussion

In this study, we demonstrate that buckwheat FeSTAR2 is a functional homolog of *Arabidopsis* ALS3. This is evidenced by the fact that FeSTAR2 could rescue the phenotype of *als3* mutant in response to Al stress (Fig. 7). Furthermore, sequence alignment analysis showed that STAR2 proteins among different plant species display high sequence similarity (Fig. 1a). In addition, in most plant species, there is only a single gene coding for STAR2 protein in their genome (Fig. 1b), suggesting the importance of functionally conserved evolution of STAR2 proteins. Consistent with our present result, it has previously been reported that buckwheat FeSTAR2/FeALS3 protein is involved in Al tolerance (Reyna-Llorens et al. 2015; Che et al. 2018). Consistent with our current finding, Che et al. (2018) also demonstrated that FeSTAR2 is homologous to

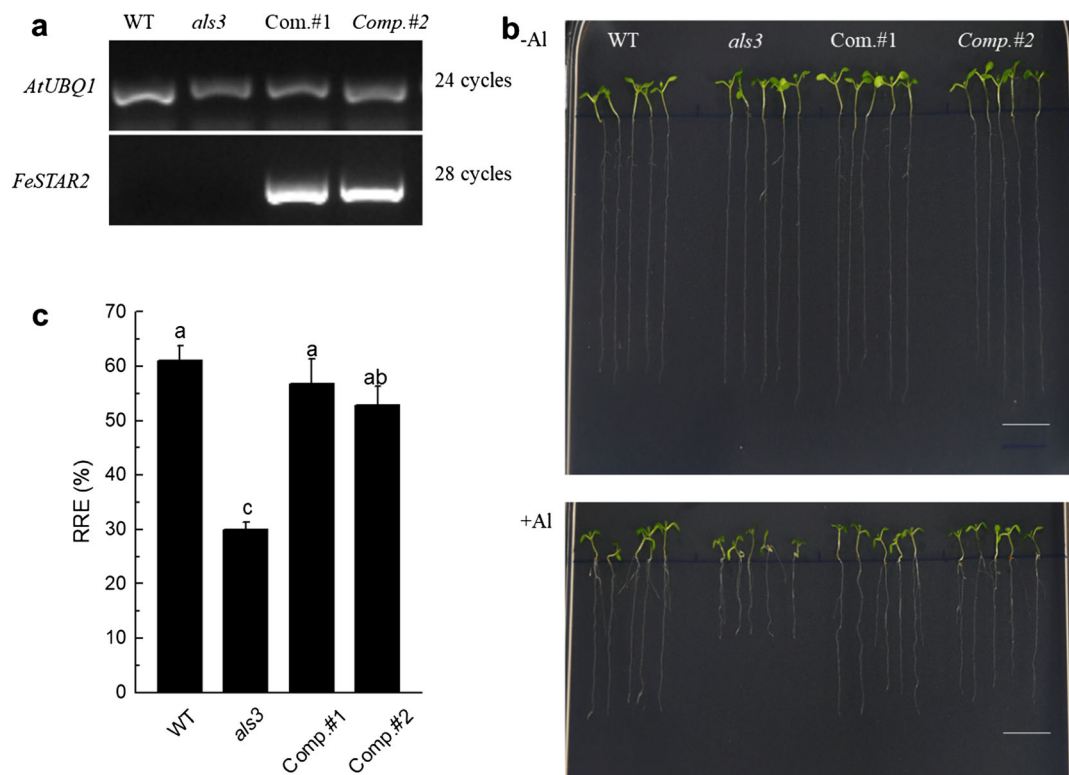


**Fig. 7** *FeSTAR2* rescues phenotype of *Arabidopsis als3* mutant in response to Al stress. **a** RT-PCR detection of *FeSTAR2* expression in WT, *als3*, and two complemented lines. **b** Phenotype of WT, *als3* and two complemented transgenic lines with or

without Al (300  $\mu$ M) stress for 7 days. **c** Relative root elongation (RRE) of seedlings in response to Al for 7 days. Data are means  $\pm$  SD ( $n=24$ ). Different letters indicate significant differences at  $P<0.05$  by Tukey test

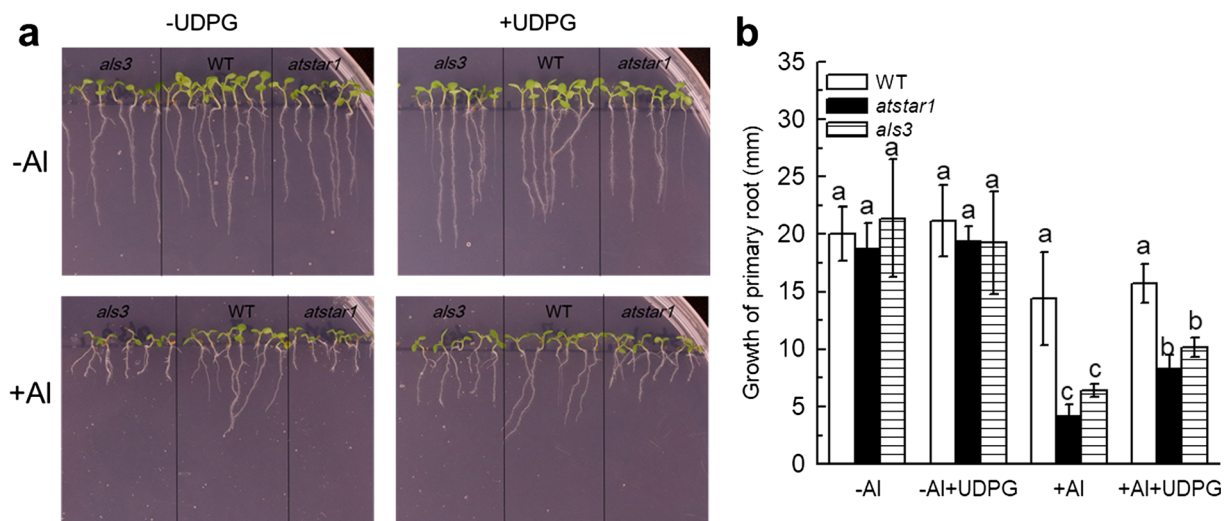


**Fig. 8** Exogenous UDP-glucose partially rescues phenotype of *als3* under Al stress. **a** The effect of exogenous UDP-glucose on the phenotype of WT and *als3* mutants under Al stress. UDP-glucose was added or not to the 1/2 MS medium (Pi concentration reduced to 100  $\mu$ M, pH 4.5, solid with 0.8% agar) containing 0 or

300  $\mu$ M Al for a week. **b** Primary root length of seedlings in (a). The primary root length was measured with a ruler after treatment. Data are means  $\pm$  SD ( $n=8$ ). Different letters indicate significant differences at  $P<0.05$  by Tukey test

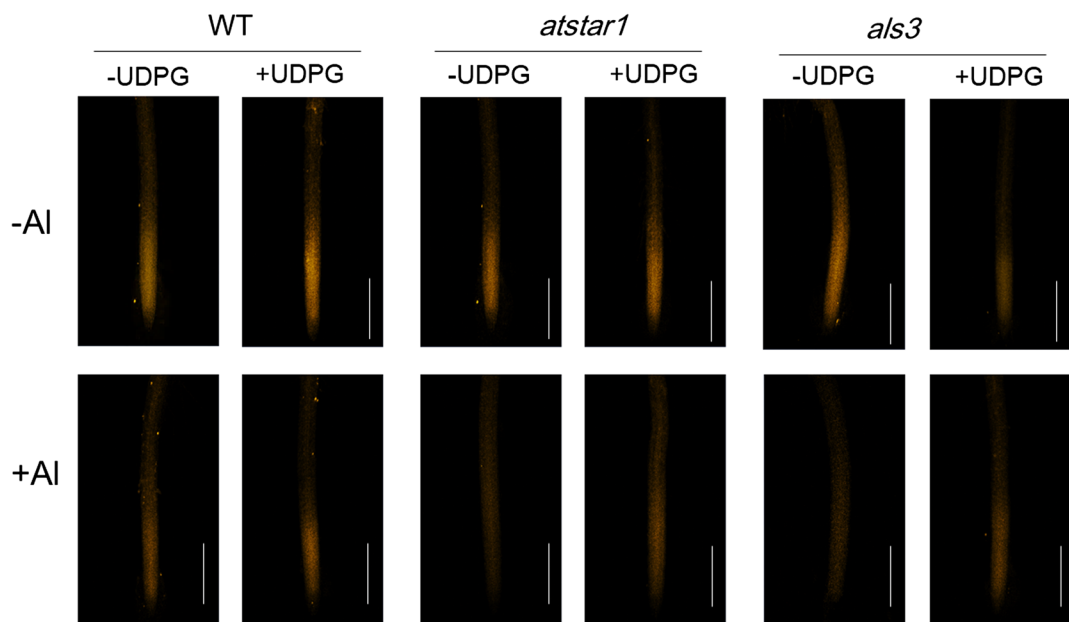


**Fig. 9** AtSTAR1 and ALS3 are positively involved in UDP-glucose-mediated XET activity. One week-old seedlings grown on plates were subjected to 0.5 mM CaCl<sub>2</sub> solution containing 0 or 50 µM Al for 24 h. Orange fluorescence shows XET activity. Bar = 200 µm

Arabidopsis ALS3. However, the exact function of FeSTAR2 remains unclear. Here, we further revealed that involvement of FeSTAR2 in Al tolerance is related to UDP-glucose metabolism (Fig. 8), which is consistent with previous study in rice in which exogenous UDP-glucose could alleviate Al-induced root growth inhibition in *osstar2* mutant (Huang et al. 2009).

In rice and Arabidopsis, knockout either STAR1 or STAR2/ALS3 resulted in hypersensitivity to Al, and STAR1 and STAR2/ALS3 could interact to form an ABC transporter protein (Huang et al. 2009, 2010; Larsen et al. 2005). Here, we demonstrate that the role of FeSTAR2 with respect to Al tolerance is closely associated with FeSTAR1 with which FeSTAR2 interact. Our conclusion is based on the following lines of evidence. First, the expression pattern was similar between FeSTAR1 and FeSTAR2 in response to Al stress (Fig. 2; Xu et al. 2018), which provides the basis for their interaction. Second, FeSTAR1 and FeSTAR2 could physically interact with each other to form a complex protein (Fig. 4). This conclusion coincides with recent report (Che et al. 2018). Finally, exogenous UDP-glucose could alleviate Al-induced root growth inhibition both in *atstar1* mutant and *als3* mutant (Fig. 8), indicating that a similar mechanism associated with UDP-glucose is employed by both STAR1 and STAR2 proteins to regulate Al tolerance.

We previously demonstrated that the involvement of STAR1 protein in Al tolerance is associated with HC metabolism (Xu et al. 2018). HC contributes significantly to Al adsorption to cell walls (Yang et al. 2011b). In this present study, we further demonstrated that STAR1 and STAR2 proteins are positively involved in the expression of XET activity (Fig. 9). XET activity is critical for HC metabolism (Rose et al. 2002). This may explain why *atstar1* mutant has higher HC1 content (Xu et al. 2018) because it has lower XET activity in comparison with WT plants (Fig. 9). However, it has to be investigated how UDG-Glucose could affect XET activity.

It is interesting to note that the subcellular location of FeSTAR1 and FeSTAR2 was changed when they form a complex protein. FeSTAR1 is a soluble protein (Xu et al. 2018), whereas FeSTAR2 is localized to biomembranes (Fig. 3). However, the complex protein of FeSTAR1 and FeSTAR2 is localized to plasma membrane and vesicles (Fig. 5). At present, the localization of STAR1 and STAR2 protein remains controversial. For example, the complex of OsSTAR1 and OsSTAR2 was reported to be localized to vesicles (Huang et al. 2009). However, Dong et al. (2017) reported that the complex of AtSTATR1 and ALS3 was largely localized to tonoplast. Considering exogenous UDP-glucose could recover the phenotype of mutants under Al stress, it is possible that the complex protein of FeSTAR1 and

FeSTAR2 is involved in vesicular transport of UDP-glucose to plasma membrane for exocytosis to modify cell walls. Consistently, our recent finding that *atstar1* mutant had higher hemicellulose1 content supports this supposition (Xu et al. 2018).

In rice, the complex protein of OsSTAR1 and OsSTAR2 form a bacterial-type ABC transporter, which is able to transport UDP-glucose to apoplast in which UDP-glucose modifies cell walls thereby preventing Al binding to cell walls (Huang et al. 2009). In the present study, we found that exogenous applied UDP-glucose could alleviate Al-induced root growth inhibition in *als3* mutant (Fig. 8). FeSTAR1 and FeSTAR2 could interact to form a bacterial-type ABC transporter (Fig. 4) and the complex protein seems to be localized to plasma membrane and vesicle membrane (Figs. 5 and 6). These results suggest that buckwheat FeSTAR1 and FeSTAR2 regulates Al tolerance by means of a mechanism similar to that employed by rice OsSTAR1 and OsSTAR2.

It appears that STAR1 and STAR2 mediated Al tolerance is a conserved mechanism in plants because they are necessary for Al tolerance in different plant species (Larsen et al. 2005; Huang et al. 2009, 2010; Reyna-Llorens et al. 2015; Che et al. 2018). However, the expression regulation mechanisms differ among different plant species. For example, while the expression of rice *OsSTAR1* and *OsSTAR2* and buckwheat *FeSTAR1* and *FeSTAR2* was induced by Al, only the expression of *ALS3* but not AtSTAR1 was induced in Arabidopsis (Larsen et al. 2005; Huang et al. 2009, 2010; Xu et al. 2017). The tissue expression pattern also differs. For example, not only in roots but also in leaves, the expression of *FeSTAR1* and *FeSTAR2* was induced by Al (Chen et al. 2017; Xu et al. 2017, 2018). However, the expression of *ALS3*, *OsSTAR1*, and *OsSTAR2* was only induced by Al in the roots (Larsen et al. 2005; Huang et al. 2009). It is therefore interesting to investigate their differential expression regulation mechanisms in the future.

In summary, our results indicate that FeSTAR2 regulates Al tolerance through interacting with FeSTAR1 to change its subcellular location of the complex protein, which may transport UDP-glucose to regulate XET activity and thereby modifying cell wall HC metabolism.

**Acknowledgements** This work was supported financially by the Natural Science Foundation of China (31572193), 111 project (grant no. B14027), and The Chang Jiang Scholars Program (JLY). We are grateful to Prof. Dong Liu for providing us the Arabidopsis mutant *als3* seeds.

**Publisher's Note** Springer Nature remains neutral with regard to jurisdictional claims in published maps and institutional affiliations.

## References

- Che J, Yamaji N, Yokosho K, Shen RF, Ma JF (2018) Two genes encoding a bacterial-type ATP-binding cassette transporter are implicated in aluminum tolerance in buckwheat. *Plant Cell Physiol* 59:2502–2511
- Chen WW, Xu JM, Jin JF, Lou HQ, Fan W, Yang JL (2017) Genome-wide transcriptome analysis reveals conserved and distinct molecular mechanisms of Al resistance in buckwheat (*Fagopyrum esculentum* Moench) leaves. *Int J Mol Sci* 18:1859
- Dong J, Pineros MA, Li X, Yang H, Liu Y, Murphy AS, Kochian LV, Liu D (2017) An Arabidopsis ABC transporter mediates phosphate deficiency-induced remodeling of root architecture by modulating iron homeostasis in roots. *Mol Plant* 10: 244–259
- Fry SC (1997) Novel 'dot-blot' assays for glycosyltransferases and glycosylhydrolases: optimization for xyloglucan endotransglycosylase (XET) activity. *Plant J* 11:1141–1150
- Fry SC, Aldington S, Hetherington PR, Aitken J (1993) Oligosaccharides as signals and substrates in the plant cell wall. *Plant Physiol* 103:1–5
- Furukawa J, Yamaji N, Wang H, Mitani N, Murata Y, Sato K, Katsuhara M, Takeda K, Ma JF (2007) An aluminum-activated citrate transporter in barley. *Plant Cell Physiol* 48: 1081–1091
- Huang CF, Yamaji N, Mitani N, Yano M, Nagamura Y, Ma JF (2009) A bacterial-type ABC transporter is involved in aluminum tolerance in rice. *Plant Cell* 21:655–667
- Huang CF, Yamaji N, Ma JF (2010) Knockout of a bacterial-type ATP-binding cassette transporter gene, AtSTAR1, results in increased aluminum sensitivity in Arabidopsis. *Plant Physiol* 153:1669–1677
- Huang CF, Yamaji N, Chen Z, Ma JF (2012) A tonoplast-localized half-size ABC transporter is required for internal detoxification of aluminum in rice. *Plant J* 69:857–867
- Jefferson RA, Kavanagh TA, Bevan MW (1987) GUS fusions: beta-glucuronidase as a sensitive and versatile gene fusion marker in higher plants. *EMBO J* 6:3901–3907
- Klug B, Horst WJ (2010) Oxalate exudation into the root-tip water free space confers protection from aluminum toxicity and allows aluminum accumulation in the symplast in buckwheat (*Fagopyrum esculentum*). *New Phytol* 187:380–391
- Kochian LV, Hoekenga OA, Piñeros MA (2004) How do crop plants tolerate acid soils? Mechanisms of aluminum tolerance and phosphorous efficiency. *Annu Rev Plant Biol* 55:459–493
- Kumar S, Stecher G, Tamura K (2016) MEGA7: molecular evolutionary genetics analysis version 7.0 for bigger datasets. *Mol Biol Evol* 33:1870–1874
- Larsen PB, Geisler MJ, Jones CA, Williams KM, Cancel JD (2005) ALS3 encodes a phloem-localized ABC transporter-like protein that is required for aluminum tolerance in Arabidopsis. *Plant J* 41:353–363

- Lei GJ, Yokosho K, Yamaji N, Fujii-Kashino M, Ma JF (2017a) Functional characterization of two half-size ABC transporter genes in aluminium-accumulating buckwheat. *New Phytol* 215:1080–1089
- Lei GJ, Yokosho K, Yamaji N, Ma JF (2017b) Two MATE transporters with different subcellular localization are involved in Al tolerance in buckwheat. *Plant Cell Physiol* 58: 2179–2189
- Liu MY, Lou HQ, Chen WW, Pineros MA, Xu JM, Fan W, Kochian LV, Zheng SJ, Yang JL (2018) Two citrate transporters coordinately regulate citrate secretion from rice bean root tip under aluminum stress. *Plant Cell Environ* 41:809–822
- Ma JF, Hiradate S (2000) Form of aluminium for uptake and translocation in buckwheat (*Fagopyrum esculentum* Moench). *Planta* 211:355–360
- Ma JF, Hiradate S, Matsumoto H (1998) High aluminum resistance in buckwheat II. Oxalic acid detoxifies aluminum internally. *Plant Physiol* 117:753–759
- Ma JF, Zheng SJ, Matsumoto H, Hiradate S (1997) Detoxifying aluminum with buckwheat. *Nature* 390(6660):569–570
- Magalhaes JV, Liu J, Guimarães CT et al (2007) A gene in the multidrug and toxic compound extrusion (MATE) family confers aluminum tolerance in sorghum. *Nat Genet* 39: 1156–1161
- Nelson BK, Cai X, Nebenführ A (2007) A multi-color set of *in vivo* organelle markers for colocalization studies in *Arabidopsis* and other plants. *Plant J* 51:1126–1136
- Reyna-Llorens I, Corrales I, Poschenrieder C, Barcelo J, Cruz-Ortega R (2015) Both aluminum and ABA induce the expression of an ABC-like transporter gene (*FeALS3*) in the Altolerant species *Fagopyrum esculentum*. *Environ Exp Bot* 111:74–82
- Rose JKC, Braam J, Fry SC, Nishitani K (2002) The XTH family of enzymes involved in xyloglucan endotransglucosylation and endohydrolysis: current perspectives and a new unifying nomenclature. *Plant Cell Physiol* 43:1421–1435
- Shen R, Ma JF, Kyo M, Iwashita T (2002) Compartmentation of aluminium in leaves of an Al-accumulator, *Fagopyrum esculentum* Moench. *Planta* 215:394–398
- Shen R, Iwashita T, Ma JF (2004) Form of Al changes with Al concentration in leaves of buckwheat. *J Exp Bot* 55:131–136
- Tang QY, Zhang CX (2012) Data processing system (DPS) software with experimental design, statistical analysis and data mining developed for use in entomological research. *Insect Sci* 20:254–260
- Vissenberg K, Martinez-Vilchez IM, Verbelen JP, Miller JG, Fry SC (2000) In vivo colocalization of xyloglucan endotransglycosylase activity and its donor substrate in the elongation zone of *Arabidopsis* roots. *Plant Cell* 12:1229–1237
- Vissenberg K, Van Sandt V, Fry SC, Verbelen JP (2003) Xyloglucan endotransglucosylase action is high in the root elongation zone and in the trichoblasts of all vascular plants from *Selaginella* to *Zea mays*. *J Exp Bot* 54:335–344
- Wang ZQ, Li GZ, Gong QQ, Li GX, Zheng SJ (2015) *OstTCTP*, encoding a translationally controlled tumor protein, plays an important role in mercury tolerance in rice. *BMC Plant Biol* 15:123
- Xu JM, Fan W, Jin JF, Lou HQ, Chen WW, Yang JL, Zheng SJ (2017) Transcriptome analysis of Al-induced genes in buckwheat (*Fagopyrum esculentum* Moench) root apex: new insight into Al toxicity and resistance mechanisms in an Al accumulating species. *Front Plant Sci* 8:1141
- Xu JM, Lou HQ, Jin JF, Chen WW, Wan JX, Fan W, Yang JL (2018) A half-type ABC transporter FeSTAR1 regulates Al resistance possibly via UDP-glucose-based hemicellulose metabolism and Al binding. *Plant Soil* 432:303–314
- Yang XY, Yang JL, Zhou Y, Pineros MA, Kochian LV, Li GX, Zheng SJ (2011a) A *de novo* synthesis citrate transporter, *Vigna umbellata* multidrug and toxic compound extrusion, implicates in Alactivated citrate efflux in rice bean (*Vigna umbellata*) root apex. *Plant Cell Environ* 34:2138–2148
- Yang JL, Zhu XF, Peng XY, Zheng C, Li GX, Liu Y, Shi YZ, Zheng SJ (2011b) Cell wall hemicellulose contributes significantly to aluminum adsorption and root growth in *Arabidopsis*. *Plant Physiol* 155:1885–1892
- Yokosho K, Yamaji N, Ma JF (2014) Global transcriptome analysis of Al-induced genes in an Al-accumulating species, common buckwheat (*Fagopyrum esculentum* Moench). *Plant Cell Physiol* 55: 2077–2091
- Yokosho K, Yamaji N, Mitani-Ueno N, Shen RF, Ma JF (2016) An aluminum inducible IREG gene is required for internal detoxification of aluminum in buckwheat. *Plant Cell Physiol* 57:1169–1178
- Zheng SJ, Ma JF, Matsumoto H (1998) High aluminum resistance in buckwheat: I. Al-induced specific secretion of oxalic acid from root tips. *Plant Physiol* 117:745–751
- Zheng SJ, Yang JL, He YF, Yu XH, Zhang L, You JF, Shen RF, Matsumoto H (2005) Immobilization of aluminum with phosphorus in roots is associated with high aluminum resistance in buckwheat. *Plant Physiol* 138:297–303
- Zhong X, Wang ZQ, Xiao R, Cao L, Wang Y, Xie Y, Zhou X (2017) Mimic phosphorylation of a  $\beta$ C1 protein encoded by TYLCCNB impairs its functions as a viral suppressor of RNA silencing and a symptom determinant. *J Virol* 91: e00300–e00317
- Zhu H, Wang H, Zhu Y, Zou J, Zhao FJ, Huang CF (2015) Genome-wide transcriptomic and phylogenetic analyses reveal distinct aluminum-tolerance mechanisms in the aluminum accumulating species buckwheat (*Fagopyrum tataricum*). *BMC Plant Biol* 15:16